Journal of Advances in Solid and Fluid Mechanics (ASFM) 1 (2019) 1-8

Size-dependent Response of Rectangular Micro-plates Subjected to Random Base Excitation Incorporating the Packaging Effect

Amir R. Askari[1*]
[1]Department of Mechanical Engineering, Hakim Sabzevari University, Sabzevar, Iran.

(Manuscript Submitted October 6, 2018; Accepted February 28, 2019)

Abstract

The objective of the present paper was to investigate the size-dependent response of a fully clamped rectangular microplate under random base excitation. The size-dependent Kirchhoff's plate model based on the modified couple stress theory was utilized in the theoretical formulation. The equations of motion which account for the packaging effect and axial residual stresses were derived using Hamilton's principle. To find the spectral density and mean square value of the microplate deflection, the standard modal summation method was employed where the microplate mode-shapes were extracted using the extended Kantorovich method. A convergence study was conducted to find the number of modes which must be included in the response. It was found that using the first six symmetric mode-shapes for the present microplate leads to very accurate results, while the single-mode solution gives the mean square value of the response with a maximum error of 10%. Furthermore, the results revealed that the size effect on the mean square value of the mid-point deflection is usually negligible when the ratio of the plate thickness to its material length scale parameter becomes larger than 15.

***Keywords**:* Rectangular microplates, Random base excitation, Modified couple stress theory, Extended Kantorovich method.

1. INTRODUCTION

Micro-systems are usually used as sensors and actuators. Because of their small size, low power consumption and the reliability of batch fabrications, there are lots of potential applications in engineering. Recently, it has been empirically observed that the conventional continuum theory cannot predict the mechanical behavior of structures in small scales accurately [1-4]. This is due to the fact that the mechanical behavior of structures seriously depends on their characteristic size that has not been included in the classical continuum theory. To find a way of capturing the mechanical behavior in small scales, higher order elasticity theories which employ some additional material constants, the so-called length scale parameters, have been developed [5]. Amongst all the presented size-dependent theories, the modified couple stress theory (MCST) is the most common theory for investigating the small scales effect on the behavior of micro-devices [6]. That's why not only this theory employs just one additional higher-order material constant, but also it is so accurate in modelling thin micro-structures under bending loads [7].

Due to the high stiffness and simplicity of the production procedure of fully clamped rectangular microplates, they represent major structural components of micro-sensors and actuators [8 ،9]. Therefore, many researchers have been motivated to focus on the investigation of the size-dependent mechanical behavior of such systems in the recent decade. Tsiatas [10] developed a linear size-dependent thin plate model for systems with an arbitrary shape based on the MCST. Asghari [11] extended the Tsiatas model for micro-plates undergone large deformations. Jomehzadeh et al. [12] analytically studied size-dependent free vibrations of circular and rectangular thin microplates with at least two opposite edges simply supported. Ke et al. [13] presented a similar work for thick microplates. Askari and Tahani [14] investigated size-dependent free vibrations of fully clamped rectangular microplates employing the Extended Kantorovich method (EKM). Zhang et al. [15] developed a size-dependent and compatible rectangular plate element with four nodes and 60-DOFs (degrees of freedoms) to investigate static bending, buckling and free vibrations of thick microplates. Thai and Choi [16] analytically investigated the non-linear behavior of FG (functionally graded) thick microplates with simply supported boundary conditions. Şimşek and Aydin [17] investigated the effect of size on the forced vibration response of an imperfect FG thick microplate under a moving load.

Micro-systems can be exposed to any undesirable forces during fabrication, deployment and operation. Hence, one of the most important issues associated with micro-devices is protecting them against undesirable environmental forces. Since the environmental forces applied to micro-systems during the transportations have a random nature, they cannot be considered as deterministic ones. So, it is essential to account for the statistical properties of these forces in designing micro-systems. However, according to the best of author's knowledge, the response of such systems under the environmental forces has not been investigated through the statistical point of view to date. Therefore, the main goal of the present paper was to investigate the

[*] Corresponding author. Tel.: +98-51-44012809; fax: +98-51- 44012607.
E-mail address: ar.askari@hsu.ac.ir and amaskari@gmail.com.

statistical properties of the response of a fully clamped rectangular microplate under a random base excitation.

Since using packages for micro-systems is unavoidable [18], the present model described the size-dependent behavior of a microplate attached to a package, where the whole system was exposed to random base excitation. In this study, Hamilton's principle played a crucial rule in deriving the equations of motion. The spectral density and mean square value of the microplate deflection were obtained through the standard modal summation method where the linear mode-shapes of the system were extracted using the EKM. A convergence study was then performed to find the number of modes which should be included in the standard modal summation method. It was found that the results would be converged if the first six symmetric mode-shapes of the present microplate were utilized. However, employing only one mode for obtaining the results would lead to the maximum error of 10%. Finally, to investigate the influences of micro-system packaging and couple stress components on the micro-plate motion, a parametric study had also been carried out. The results revealed that the existence of the microplate package, which did not affect the influence of couple stress components, magnified the effect of base excitation. Hence, selecting an appropriate package which can minimize this increasing effect is so essential.

2. PROBLEM FORMULATION

Fig. 1 depicts a schematic of a clamped microplate attached to a package, which is modelled as a lumped mass, under a random base excitation $Z(t)$. It is assumed that the microplate density is denoted by *ρ*, also *a*, *b* and *h* are the length, width and thickness of the system. The initial gap between the un-deformed plate and the fixed substrate is *d*. Furthermore, *x*, *y* and *z* are the coordinates along the length, width and thickness, respectively.

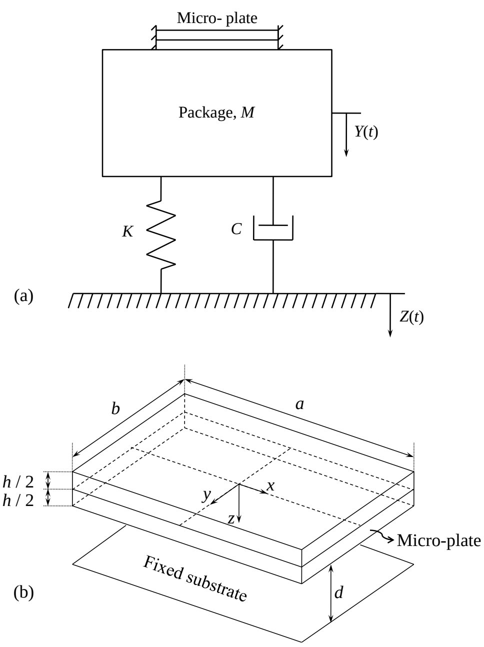

Fig. 1. Schematic of a rectangular micro-plate and its package.

Employing the Hamilton principle, the governing equations of motion for the present system based on the size-dependent Kirchhoff plate theory [14] take the form

$$I_0\ddot{w} - I_2\nabla^2\ddot{w} + \left(\frac{Eh^3}{12\left(1-\nu^2\right)} + \frac{Ehl^2}{2\left(1+\nu\right)}\right)\nabla^4 w - N_x^r\frac{\partial^2 w}{\partial x^2} - N_y^r\frac{\partial^2 w}{\partial y^2} = -I_0\left(\ddot{W}+\ddot{Z}\right) \quad (1a)$$

$$\left(M+m\right)\ddot{W} + C\dot{W} + KW + \int_A I_0\ddot{w}\,dA = -\left(M+m\right)\ddot{Z} \quad (1b)$$

where w is the micro-plate deflection and $W=Y-Z$. Also, *E*, ν and *l* are the elasticity modulus, Poison's ratio and the material length scale parameter of the microplate, respectively. *M*, *K* and *C*, respectively, denote the mass, stiffness and damping of the package. *m* is the total mass of the microplate ($m=\rho abh$). Also, the mass inertias (I_0,I_2) are defined by

$$\left(I_0,I_2\right)=\int_{-h/2}^{h/2}\rho\left(1,z^2\right)dz=\rho\left(h,\frac{h^3}{12}\right) \quad (2)$$

N_x^r and N_y^r are the resultant axial residual forces per unit length applied to the microplate due to the mismatch of both thermal expansion coefficient and crystal lattice period between the substrate and microplate film [19].

Due to the slenderness of MEMS microplates, the rotary inertia is negligible in comparison to the translatory one [20]. Hence, the term $I_2\nabla^2\ddot{w}$ in Eq. (1a) can simply be neglected. Furthermore, the effect of the microplate mass on the package motion can also be neglected, because of its smallness in comparison to the packaging mass. Employing the dimensionless variables $\hat{x}=\frac{x}{a}$, $\hat{y}=\frac{y}{b}$, $\hat{w}=\frac{w}{d}$, $\hat{t}=\frac{t}{T}$, $\hat{W}=\frac{W}{d}$ and $\hat{Z}=\frac{Z}{d}$, the normalized form of the governing equations of motion can be obtained as:

$$\ddot{w}+\bar{c}\dot{w}+\bar{k}w=-\ddot{z} \quad (3a)$$

$$\ddot{w}+\left[\frac{1+6\alpha_2}{12}\right]\left[\frac{\partial^4 w}{\partial x^4}+2\alpha_1^2\frac{\partial^4 w}{\partial x^2 y^2}+\alpha_1^4\frac{\partial^4 w}{\partial y^4}\right]-N_1\frac{\partial^2 w}{\partial x^2}-N_2\frac{\partial^2 w}{\partial y^2}=-(\ddot{w}+\ddot{z}) \quad (3b)$$

The time scale of the problem (i.e. *T*) has also been chosen such that the coefficient of $\ddot{w}$ in Eq. (3a) becomes unity. Therefore, the normalized parameters of the system are given by:

$$\alpha_1 = \frac{a}{b} \quad , \quad \alpha_2 = \frac{1-v}{(h/l)^2}, \quad N_1 = \frac{\alpha^2(1-v^2)}{Eh^3} N_x^r \ ,$$
$$N_2 = \frac{\alpha^4(1-v^2)}{Eh^3 b^2} N_y^r \quad , \quad \bar{c} = \frac{CT}{M} = 2\mathrm{T}\zeta_P \omega_P \ , \tag{4}$$
$$\bar{k} = \frac{kT^2}{M} = T^2 \omega_p^2$$

in which ξ_p and ω_p represent the damping ratio and natural frequency of the package, respectively. The dimensionless form of the clamped boundary conditions for the present problem takes the form of

$$\mathrm{w}\ (\mathrm{x,y,t}) \big|_{x=-\frac{1}{2},\frac{1}{2}} = \mathrm{w}\ (\mathrm{x,y,t}) \big|_{x=-\frac{1}{2},\frac{1}{2}} = 0$$
$$\mathrm{w}\ (\mathrm{x,y,t}) \big|_{y=-\frac{1}{2},\frac{1}{2}} = \mathrm{w}\ (\mathrm{x,y,t}) \big|_{y=-\frac{1}{2},\frac{1}{2}} = 0 \tag{5}$$

Furthermore, it was assumed that the microplate and its package became at rest before applying the random base excitation $Z(t)$. Hence, one can write

$$w(x,y,t)\big|_{t=0} = \dot{w}(x,y,t)\big|_{t=0}$$
$$= W(t)\big|_{t=0} = \dot{W}(t)\big|_{t=0} = 0 \tag{6}$$

3. RESPONSE TO THE RANDOM BASE EXCITATION

In the present paper, the response of the microplate to the random base excitation $Z(t)$ will be obtained using the standard modal summation method. Based on the standard modal summation method [21] one can write

$$w(x,y,t) = \sum_{m=1}^{\infty}\sum_{n=1}^{\infty} \psi_{mn}(x,y)\,\zeta_{mn}(t) \tag{7}$$

where $\psi_{mn}(x,y)$ and $\zeta_{mn}(t)$ are called the mode-shape and its associated general coordinate of the system, respectively. Since analytical solutions for microplate mode-shapes are only available for plates with at least one pair of opposite edges simple supported, herein, the mode-shapes of the present fully clamped microplate are obtained using the EKM [14].

According to the EKM, the variational form of the eigenvalue problem associated with Eq. (3a) is considered. Then, the microplate mode-shapes are assumed to be a multiplication of single term separable functions. Afterward, according to the iterative nature of the EKM, at the first step, it is assumed that one of the separated functions to be prescribed and known and selected as an arbitrary function which satisfies all its associated kinematic boundary conditions. Therefore, the variation of the microplate mode-shapes would be just because of the variation of the other un-known separated function. Doing so and employing the fundamental lemma of variational calculus, the variational form of the eigenvalue problem associated with Eq. (3a) can simply be re-written as an ordinary differential equation in terms of the un-known separated function. Solving this boundary value problem, one can obtain the un-known separated function. Afterward, by continuing the iterative procedure of the EKM, one can utilize the obtained separated function as a prescribed function and find the other separated function guessed at the first step. The procedure should be continued until the convergence occurs. It is to be noted that, the convergence of the EKM is so fast, that usually, one iterate is sufficient to find a very accurate solution [14]. To find more details about the application of the EKM in determining fully clamped rectangular microplates mode-shapes, see our previous work [14].

Obtaining linear mode-shapes of the present micro-plate, herein, the governing equation of motion will be discretized into the modal equations using the standard modal summation method. To do so, one can substitute Eq. (7) into Eq. (3a), multiplying both sides of the resulting equation by $\psi_{ij}(x,y)$, employing the orthogonality of the determined linear mode-shapes [14] and obtain

$$\ddot{\zeta}_{ij}(t) + \omega_{ij}^2 \zeta_{ij}(t) = \frac{F_{ij}(t)}{M_{ij}} \tag{8}$$

Where

$$M_{ij} = \int_{-1/2}^{1/2}\int_{-1/2}^{1/2} \psi_{ij}^2 \ dxdy \tag{9a}$$

$$F_{ij}(t) = -(\ddot{W} + \ddot{Z})\int_{-1/2}^{1/2}\int_{-1/2}^{1/2} \psi_{ij} \ dxdy \tag{9b}$$

3.1. SPECTRAL DENSITY AND EXPECTED SQUARE VALUE OF THE RESPONSE

According to Eqs. (3), it is apparent that one needs to obtain the spectral density of the package response (i.e. $W(t)$) in terms of $S_{\ddot{Z}}(\omega)$ as the input of Eq. (3b). Doing so, the spectral density of the microplate response would be obtained by finding the spectral density of $-(\ddot{W} + \ddot{Z})$.

According to the single-input-single-output (SISO) Eq. (3b), the spectral density of $W(t)$ takes the form [22]

$$S_W(\omega) = |H(\omega)|^2 S_{\ddot{Z}}(\omega) \tag{10}$$

$$H(\omega) = \frac{1}{(\omega^2 - T^2\omega_p^2) - i(2\xi_p T\omega_p\omega)} \tag{11}$$

To find, $S_{-(\ddot{W}+\ddot{Z})}(\omega)$ a new variable $\Theta(t)=-(\ddot{W}+\ddot{Z})$ is introduced. Doing so, according to Eq. (3b), the auto-correlation function for $\Theta(t)$ can be written as [22]

$$R_\Theta(\tau)=E[\Theta(t)\Theta(t+\tau)]=E[\{(2T\zeta_P\omega_P)\dot{W}(t)+(T^2\omega_p^2)W(t)\}\{(2T\zeta_P\omega_P)\dot{W}(t+\tau)+(T^2\omega_p^2)W(t+\tau)\}] \quad (12)$$

Which can also be simplified to:

$$R_\Theta(\tau)=4T^2\xi_p^2\omega_p^2R_{\dot{W}}(\tau)+2T^3\xi_p\omega_p^3\left[R_{\dot{W}W}(\tau)+R_{W\dot{W}}(\tau)\right]+T^4\omega_p^4R_W(\tau) \quad (13)$$

The spectral density of $\Theta(t)$ (i.e. $S_\Theta(\omega)$) can also be found through obtaining the Fourier transform of the auto-correlation function of $\Theta(t)$ as [22]

$$S_\Theta(\omega)=4T^2\xi_p^2\omega_p^2S_{\dot{W}}(\omega)+2T^3\xi_p\omega_p^3\left[S_{\dot{W}W}(\omega)+S_{W\dot{W}}(\omega)\right]+T^4\omega_p^4S_W(\omega) \quad (14)$$

where the spectral density of $\dot{W}(t)$ takes the form [22]

$$S_{\dot{W}}(\omega)=\omega^2S_W(\omega) \quad (15)$$

To complete the procedure of finding $S_\Theta(\omega)$, it is sufficient to determine $S_{\dot{W}W}(\omega)$ and $S_{W\dot{W}}(\omega)$ for the present stationary and ergodic process. To do so, using the auto-correlation function of $W\dot{W}$ and $\dot{W}W$, one can write [22]

$$R_{W\dot{W}}(\tau)=E\left[W(t)\dot{W}(t+\tau)\right]=\frac{d}{d\tau}R_W(\tau)=\frac{d}{d\tau}\left(\int_{-\infty}^{+\infty}S_W(\omega)\exp(i\omega\tau)d\omega\right)=\int_{-\infty}^{+\infty}i\omega S_W(\omega)\exp(i\omega\tau)d\omega \quad (16a)$$

$$R_{W\dot{W}}(\tau)=E\left[W(t)\dot{W}(t+\tau)\right]=\frac{d}{d\tau}R_W(\tau)=\frac{d}{d\tau}\left(\int_{-\infty}^{+\infty}S_W(\omega)\exp(i\omega\tau)d\omega\right)=\int_{-\infty}^{+\infty}i\omega S_W(\omega)\exp(i\omega\tau)d\omega \quad (16b)$$

It is to be noted that Eqs. (16) are derived using the fact that the auto-correlation function is even and the process is stationary. According to these equations, the spectral density of $W\dot{W}$ and $\dot{W}W$ can be obtained by employing the inverse Fourier transform. Doing so, one would get

$$S_{W\dot{W}}(\omega)=i\omega S_W(\omega) \quad (17a)$$

$$S_{\dot{W}W}(\omega)=-i\omega S_W(\omega) \quad (17b)$$

Therefore, using Eqs. (10), (14), (15), and (17), the spectral density of $\Theta(t)$ can be obtained as

$$S_\Theta(\omega)=\left(4T^2\xi_p^2\omega_p^2\omega^2+T^4\omega_p^4\right)S_W(\omega)=\frac{4T^2\xi_p^2\omega_p^2\omega^2+T^4\omega_p^4}{\left(\omega^2-T^2\omega_p^2\right)^2+\left(2\xi_pT\omega_p\omega\right)^2}S_{\ddot{Z}}(\omega) \quad (18)$$

As the last step, according to Eq. (8), the spectral density of the microplate response (i.e.$S_w(x,y,\omega)$) can be determined as [22]

$$S_w(x,y,\omega)=S_\Theta(\omega)\sum_{i=1}^{\infty}\sum_{j=1}^{\infty}\sum_{m=1}^{\infty}\sum_{n=1}^{\infty}\psi_{ij}(x,y)\psi_{mn}(x,y)H_{ij}(\omega)H_{mn}^*(\omega)=\frac{\left(4T^2\xi_p^2\omega_p^2\omega^2+T^4\omega_p^4\right)}{\left\{\left(\omega^2-T^2\omega_p^2\right)^2+\left(2\xi_pT\omega_p\omega\right)^2\right\}}S_{\ddot{Z}}(\omega)\sum_{i=1}^{\infty}\sum_{j=1}^{\infty}\sum_{m=1}^{\infty}\sum_{n=1}^{\infty}\psi_{ij}(x,y)\psi_{mn}(x,y)\times H_{ij}(\omega)H_{mn}^*(\omega) \quad (19)$$

where $H_{ij}(\omega)$ is the frequency response function of the output $\zeta_{ij}(t)$ under the input $\Theta(t)$ and can be obtained through SISO Eq. (8) as

$$H_{ij}(\omega)=\frac{\int_{-1/2}^{1/2}\int_{-1/2}^{1/2}\psi_{ij}\,dxdy}{\int_{-1/2}^{1/2}\int_{-1/2}^{1/2}\psi_{ij}^2\,dxdy}\times\frac{1}{\left(-\omega^2+\omega_{ij}^2\right)} \quad (20)$$

It is to be noted that $H^{*}_{ij}(\omega)$ also denotes the complex conjugate of $H_{ij}(\omega)$ which equals to $H_{ij}(\omega)$ for the present problem.

To find the expected square value of the microplate response one can write [22]

$$E\left[w^2\right]=\int_{-\infty}^{+\infty} S_w(x,y,\omega)\,d\omega \qquad (21)$$

It was worth noting that the aforementioned relations were obtained for any desirable stationary and ergodic random input of the problem. To provide some numerical results, herein, it was assumed that the input signal to be a practical stationary and ergodic white noise with spectral density shown in Fig. 2. In this case, the expected square value of the microplate response can be simplified to

$$E\left[w^2\right]=\frac{S_0T^2}{2\pi d^2}\sum_{i=1}^{\infty}\sum_{j=1}^{\infty}\sum_{m=1}^{\infty}\sum_{n=1}^{\infty} C_{ij} C_{mn}\psi_{ij}(x,y)\psi_{mn}(x,y) \int_0^{2\pi T\omega_0}\frac{A(\omega)}{\left(-\omega^2+\omega_{ij}^2\right)\left(-\omega^2+\omega_{mn}^2\right)}d\omega \qquad (22)$$

where:

$$C_{ij}=\frac{\int_{-1/2}^{1/2}\int_{-1/2}^{1/2}\psi_{ij}\,dxdy}{\int_{-1/2}^{1/2}\int_{-1/2}^{1/2}\psi_{ij}^2\,dxdy} \qquad (23a)$$

$$A(\omega)=\frac{4T^2\xi_p^2\omega_p^2\omega^2+T^4\omega_p^4}{\left(\omega^2-T^2\omega_p^2\right)^2+\left(2\xi_pT\omega_p\omega\right)^2} \qquad (23b)$$

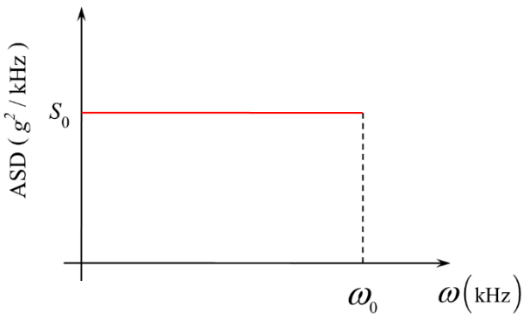

Fig.2. One-sided acceleration spectral density (ASD) of the excitation.

4. RESULTS AND DISCUSSION

4.1. CONVERGENCE INVESTIGATION

To investigate the convergence of the present standard modal summation method, an un-stressed square silicon microplate with material and geometric properties presented in Table 1 was considered. Table 2 and Fig. 3 investigated the convergence of both the classical and size-dependent mean square value as well as the spectral density of the microplate mid-point deflection for a typical system with $\xi_p=0.02$, $\omega_p=10$ kHz, $\omega_0=15$ kHz, $S_0=1\,g^2/\text{kHz}$, respectively [23-26]. It is to be mentioned here that, according to Eq. (22), only symmetric modes affect the microplate motion. Hence, only symmetric modes are included in the present analysis.

Table 1. Geometric and material properties of an unstressed square micro-plate made of 110-direction silicon [6].

a (μm)	h (μm)	d (μm)	E (GPa)
100	1	1	169
ν	ρ (kg/m^3)	l (μm)	
0.3	2332	0.592	

Table 2. Convergence of the dimensionless mid-point deflection mean square values versus the number of included symmetric modes for the present micro-plate.

	Number of modes								
	1	2	3	4	5	6	7	8	9
CT	13.5	12.7	12.	12.13	12.10	12.09	12.09	12.09	12.09
MCST	2.21	2.09	1.97	1.98	1.98	1.98	1.98	1.98	1.98

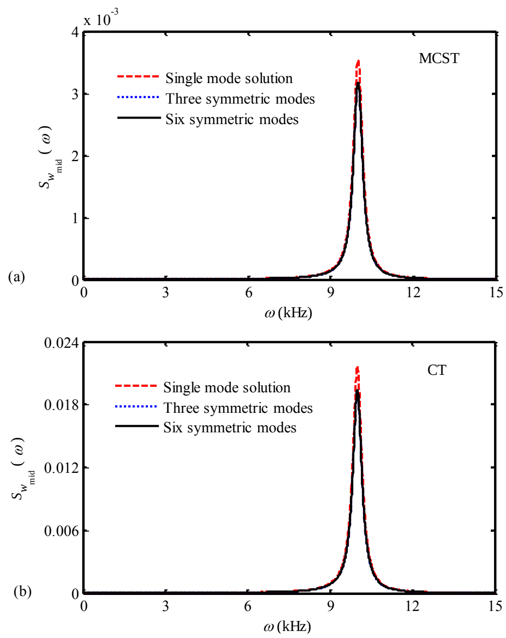

Fig. 3. Dimensionless and one-sided spectral density of the micro-plate mid-point deflection.

In view of Table 2 and Fig. 3, it was obvious that if the first six symmetric modes were employed in the present analysis, the results would completely be converged. However, using single-mode solution gives the maximum error of 10%. Therefore, despite the good accuracy of the single-mode solution, the present results would be obtained through a six modes approximation, hereinafter.

According to the results of Fig. 3, it is obvious that if the practical white noise frequencies cover the natural frequency of the package, the spectral density of the micro-plate mid-point deflection will be increased. Therefore, due to the fact that packing is unavoidable, it is essential to select a package with a natural frequency larger than those covered by the practical white noise input. Also, It should be mentioned here that since most of the micro-devices enjoy very large natural frequencies (for example the classical first natural frequency of the present microplate becomes 1.476 MHz [14]) in comparison to the natural frequency of the package and those of the input, the problem of covering the natural frequencies of the microplate by the input frequencies will not be raised.

4.2. EFFECT OF SMALL SCALES

According to the results of Table 2 and Fig. 3, neglecting the effect of couple stress components, respectively, may lead to an overestimation of the mean square values and spectral density of the present microplate mid-point deflections. To investigate this issue more, Fig. 4 depicted the variation of ESV/ESV$_0$ (where ESV denotes the expected square value of the mid-point deflection calculated through the MCST and ESV$_0$ refers to those evaluated using the CT) versus the size effect parameter (*h*/*l*) for the present system. As it can be observed from Fig. 4, accounting for the effect of couple stress components increases the bending rigidity of the microplate which results in the reduction of the values of the microplate mid-point deflections. In addition, increasing the size-effect parameter (i.e. *h*/*l*) decreases the influence of small scales such that this effect becomes negligible for microplates with the ratio of plate thickness to its material length scale parameter larger than 15. It is worth mentioning that since Poisson's ratio is about 0.3 for most of the engineering materials, this conclusion can easily be extended to most of plate-based micro-systems. Especially that, as it can be observed from Fig. 4, the ASD of the input as well as the package characteristics do not affect the ratio of ESV/ESV$_0$.

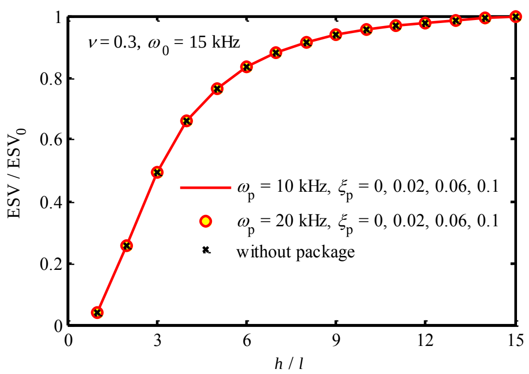

Fig. 4. The ratio of the dimensionless expected square values (ESV) of the micro-plate mid-point deflection calculated through the MCST to those obtained using the CT versus the size effect parameter (h/l).

4.3. EFFECT OF PACKAGING

To investigate the influence of microplate packaging on its motion, Fig. 5 depicted the dimensionless and one-sided spectral density of the mid-point deflection for a silicon microplate with properties presented in Table 1, $\xi_p = 0.02$ and $\omega_p = 10, 20 \text{ and } 30 \text{ kHz}$, using both the CT and the MCST. The maximum frequency and spectral density of the practical white noise input are also assumed to be $\omega_0 = 15\,\text{kHz}$, $S_0 = 1\,g^2/\text{kHz}$, respectively. For the sake of improving the state of presentation, the results of Fig. 5 are separated to those related to $\omega_p = 10\,\text{kHz}$ and $\omega_p = 20, 30\,\text{kHz}$, respectively, plotted in Figs. 5(a) and 5(b). According to Figs. 5, it is obvious that neglecting the effect of couple stresses may lead to very inaccurate results. Furthermore, as these figures depicted, if the input frequencies do not cover the natural frequency of the package, the spectral density of the response may drastically be decreased. So, selecting a package with the natural frequency out of the input frequencies interval will be considered as a smart choice.

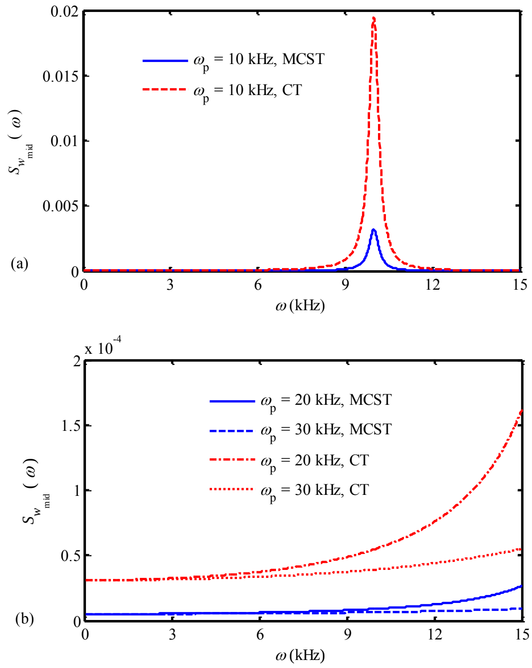

Fig. 5. Dimensionless and one-sided spectral density of the mid-point deflection for the present micro-plate.

Herein, the spectral density and expected square value of the response are derived for a system with no package. Doing so will provide us with a deep point of view about the role of microplate the packaging in its motion. However, since packaging is unavoidable in micro-system assemblies, it represents a wrong case scenario. The spectral density for a system without the package takes the form

$$S_w(x,y,\omega)= S_{\ddot{Z}}(\omega)\sum_{i=1}^{\infty}\sum_{j=1}^{\infty}\sum_{m=1}^{\infty}\sum_{n=1}^{\infty}\psi_{ij}(x,y)\psi_{mn}(x,y)H_{ij}(\omega) H^*_{mn}(\omega) \quad (24)$$

The expected square value of the response can also be written as :

$$E\left[w^2\right]=\int_{-\infty}^{+\infty}S_w(x,y,\omega)\,d\omega \quad (25)$$

This value for the present practical stationary and ergodic white noise with one-sided spectral density presented in Fig. 2 can be simplified to

$$E\left[w^2\right]=\frac{S_0T^2}{2\pi d^2}\sum_{i=1}^{\infty}\sum_{j=1}^{\infty}\sum_{m=1}^{\infty}\sum_{n=1}^{\infty}C_{ij}C_{mn}\psi_{ij}(x,y) \psi_{mn}(x,y)\int_0^{2\pi T\omega_0}\frac{1}{\left(-\omega^2+\omega_{ij}^2\right)\left(-\omega^2+\omega_{mn}^2\right)}d\omega \quad (26)$$

Fig. 6 depicts the spectral density of the mid-point deflection for the present microplate without the packaging effect using the MCST. Comparing this figure with Figs. 5(a) and 5(b) demonstrates that accounting for the influence of packaging may magnify the spectral density of the response which means that the microplate mid-point deflection takes larger values. Hence, it is very essential to account for the packaging effect in designing microsystems.

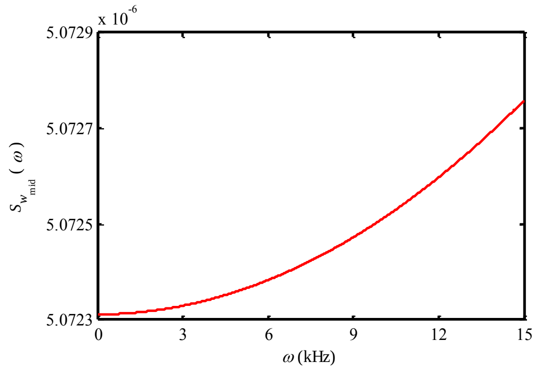

Fig. 6. Dimensionless and one-sided spectral density of the mid-point deflection for the present silicon micro-plate without the packaging effect.

As Figs. 5 and 6 depict, accounting for the packaging effect increases the spectral density of the response which leads to an increase in the mean square value of the micro-plate deflection. Hence, it is essential to design an appropriate package for the system to minimize the increasing effect of the micro-plate packaging on its deflection. To investigate this issue more, Fig. 7 depicts the variation of the dimensionless mean square value of the mid-point deflection for the present silicon microplate under a practical white noise with $S_0 = 1\,g^2/\text{kHz}$ and $\omega_0 = 15$ kHz versus the variation of the natural frequency of the package for a system with $\xi_p = 0.02$. It is to be noted that the dimensionless mean square value of mid-point deflection for the present micro-plate without the package is calculated as 0.076.

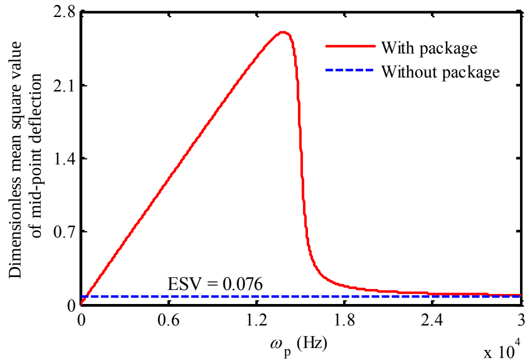

Fig. 7. Variation of mean square values of the mid-point deflection for the present micro-plate versus the variation of the natural frequency of the package.

As Fig. 7 depicts, the increasing effect of the microplate packaging will be minimized if the natural frequency of the package is selected far from those covered by the input. It is to be noted that, for the case at hand, if it is not possible to choose a package with a natural frequency larger than those covered by the input, the damping ratio of the package should be increased. Fig. 8 illustrates the effect of the damping ratio on the mean square value of the microplate mid-point deflection for the present system. As it can be observed from this figure, increasing the package damping ratio, drastically decrease the microplate deflection. However, selecting a package with very large damping will result in the increase of the transferred force to the board on which the micro-system has been attached. Hence, this issue should also be taken in the mind during the packaging design.

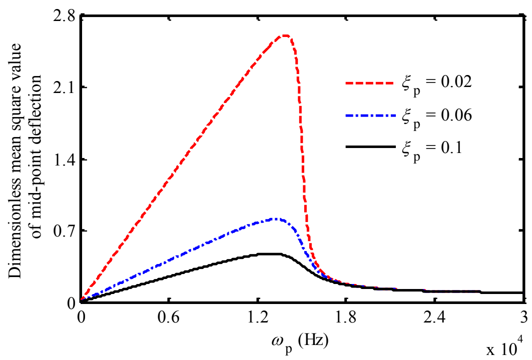

Fig. 8. Effect of the package damping ratio on the mean square values of the micro-plate mid-point deflection.

5. CONCLUDING REMARKS

In this paper, size-dependent spectral density and expected square value of a clamped rectangular microplate deflection were derived based on the

MCST. Hamilton's principle was employed to derive the equations of motion and the standard modal summation method was utilized to discrete the solution into the modal coordinates. The analytic mode-shapes of the present microplate were also extracted using the EKM. The spectral density of the response was found by employing the Fourier transform of the auto-correlation function of the solution. To provide some numerical results, the present findings were also simplified for a practical stationary and ergodic white noise. The results revealed that utilizing the first six symmetric modes in the standard modal summation method leads to very accurate results, while the single-mode solution suffered from only a maximum error of 10%. A parametric study was then performed to investigate the influences of couple stress components and packaging on the spectral density and mean square value of the response. It was found that accounting for the small scales effect increases the microplate bending rigidity for systems in which the ratio of the microplate thickness to its material length scale parameter takes values less than 15. In addition, it was observed that accounting for the packaging effect would magnify the microplate deflection which must be reduced through selecting an appropriate package with optimized natural frequency and damping ratio.

REFERENCES

[1] N. A. Fleck, G. M. Muller, M. F. Ashby and J. W. Hutchinson, Strain gradient plasticity: theory and experiment, Acta Metall. Mater., Vol. 42, pp. 475–487, 1994.

[2] J. S. Stölken and A. G. Evans, Microbend test method for measuring the plasticity length scale, Acta Mater., Vol. 46, pp. 5109-5115, 1998.

[3] A. C. M. Chong and D. C. C. Lam, Strain gradient plasticity effect in indentation hardness of polymers, J. Mater. Res. , Vol. 14, pp. 4103-4110, 1999.

[4] A. W. McFarland and J. S. Colton, Role of material microstructure in plate stiffness with relevance to microcantilever sensors, J. Micromech. Microeng., Vol. 15, pp. 1060-1067, 2005.

[5] M. Hosseini, A. Hadi, A. Malekshahi and M. Shishesaz, A review of size-dependent elasticity for nanostructures, J. Comput. Applied Mech., Vol. 49, No. 1, pp. 197-211, 2018.

[6] M. Rahaeifard, M. H. Kahrobaiyan, M. Asghari and M. T. Ahmadian, Static pull-in analysis of microcantilevers based on the modified couple stress theory, Sensor Actuat. A-Phys. , Vol. 171, pp. 370-374, 2011.

[7] M. H. Kahrobaiyan, M. Asghari and M. T. Ahmadian, Strain gradient beam element, Finite Elem. Anal. Des. , Vol. 68, pp. 63–75, 2013.

[8] O. Français and I. Dufour, Normalized abacus for the global behavior of diaphragms: pneumatic, electrostatic, piezoelectric or electromagnetic actuation, J. Model. Simul. Microsyst., Vol. 1, No. 2, pp. 149–60, 1999.

[9] R. C. Batra, M. Porfiri and D. Spinello, Review of modeling electrostatically actuated microelectromechanical systems, Smart Mater. Struct., Vol. 16, pp. 23-31, 2007.

[10] G. C. Tsiatas, A new Kirchhoff plate model based on a modified couple stress theory, Int. J. Solids Struct., Vol. 46, pp. 2757–2764, 2009.

[11] M. Asghari, Geometrically nonlinear micro-plate formulation based on the modified couple stress theory, int. J. Eng. Sci., Vol. 51, pp. 292–309, 2012.

[12] E. Jomehzadeh, H. R. Noori and A. R. Saidi, The size-dependent vibration analysis of micro-plates based on a modified couple stress theory, Physica E, Vol. 43, pp. 877–883, 2011.

[13] L. L. Ke, Y. S. Wang, J. Yang and S. Kitipornchai, Free vibration of size-dependent Mindlin microplates based on the modified couple stress theory, J. Sound Vib., Vol. 331, pp. 94–106, 2012.

[14] A. R. Askari and M. Tahani, Analytical determination of size-dependent natural frequencies of fully clamped rectangular micro-plates based on the modified couple stress theory, J. Mech. Sci. Technol., Vol. 29, No. 5, pp. 2135-2145, 2015. Accepted for publication.

[15] B. Zhang, Y. He, D. Liu, Z. Gan and L. Shen, A non-classical Mindlin plate finite element based on a modified couple stress theory, Eur. J. Mech. A-Solid, Vol. 42, pp. 63-80, 2013.

[16] H. T. Thai and D. H. Choi, Size-dependent functionally graded Kirchhoff and Mindlin plate models based on a modified couple stress theory, Compos. Struct., Vol. 95, pp. 142–153, 2013.

[17] M. Şimşek and M. Aydın, Size-dependent forced vibration of an imperfect functionally graded (FG) microplate with porosities subjected to a moving load using the modified couple stress theory, Compos. Struct., Vol. 160, pp. 408-421, 2017.

[18] I. Y. Mohammad, M. A. Fadi, M. Ronald and S. Quang, Characterization of the performance of capacitive switches activated by mechanical shock, J. Micromech. Microeng., Vol. 17, No. 7, pp. 1360, 2007.

[19] J. Qian, C. Liu, D. C. Zhang and Y. P. Zhao, Residual stresses in micro-electro-mechanical system, J. Mech. Strength, Vol. 23, pp. 393-401, 2001.

[20] J. N. Reddy, Theory and Analysis of Elastic Plates and Shells, 2nd ed., Philadelphia: Taylor & Francis, 2007.

[21] S. S. Rao, Vibration of Continuous Systems, USA: John Wiley & Sons, 2007.

[22] D. E. Newland, An Introduction to Random Vibrations, Spectral & Wavelet Analysis 3rd ed., New York: Dover Publications, 2005.

[23] A. R. Askari, Non-linear Analysis of Electrically Actuated Thin Micro-Plates Based on The Modified Couple Stress Theory, PhD Thesis, Dept of Mechanical Engineering, Ferdowsi University of Mashhad, Mashhad, Iran, 2017. (in Persian)

[24] JEDEC Solid State Technology Association, JESD22-B110: Subassembly Mechanical Shock, Arlington, VA, 2001.

[25] JEDEC Solid State Technology Association, JESD22-B111: board level drop test method of components for handheld electronics products, Arlington, VA, 2003.

[26] C.-L. Yeh and Y.-S. Lai, Support excitation scheme for transient analysis of JEDEC board-level drop test, Microelectron. Reliab., Vol. 46, No. 2-4, pp. 626-636, 2006.